NIST United States Department of Commerce
National Institute of Standards and Technology

NISTIR 3964

CONTINUOUS-COOLING TRANSFORMATION CHARACTERISTICS AND HIGH-TEMPERATURE FLOW BEHAVIOR OF A MICROALLOYED SAE 1141 STEEL

Yi-Wen Cheng
Avinoam Tomer

NISTIR 3964

CONTINUOUS-COOLING TRANSFORMATION CHARACTERISTICS AND HIGH-TEMPERATURE FLOW BEHAVIOR OF A MICROALLOYED SAE 1141 STEEL

Yi-Wen Cheng
Avinoam Tomer*

Materials Reliability Division
Materials Science and Engineering Laboratory
National Institute of Standards and Technology
Boulder, Colorado 80303-3328

February 1991

*Guest researcher from Nuclear Research Center – Negev, Beer Sheva, Israel

U.S. DEPARTMENT OF COMMERCE, Robert A. Mosbacher, Secretary
NATIONAL INSTITUTE OF STANDARDS AND TECHNOLOGY, John W. Lyons, Director

CONTENTS

		Page
ABSTRACT		vii
I.	INTRODUCTION	1
II.	EXPERIMENTAL PROCEDURES	2
III.	EXPERIMENTAL RESULTS AND DISCUSSION	3
	Continuous-Cooling Transformation (CCT) Characteristics	3
	Metallography	5
	Hardness Measurements	8
	True Stress-vs.-True Strain Curves	8
	Using Recrystallization to Control Austenite Grain Size	10
IV.	SUMMARIES AND CONCLUDING REMARKS	11
V.	ACKNOWLEDGMENTS	13
VI.	REFERENCES	14

LIST OF TABLES

		Page
1.	Chemical composition of the microalloyed SAE 1141 steel (mass percent).	2
2.	Experimental conditions.	3
3.	Results of microhardness measurements.	8
4.	Values used to calculate Q and C in equation (4).	9
5.	Computed austenite grain sizes after different deformation schedules. . . .	11

LIST OF FIGURES

Page

1. The CCT diagram of the microalloyed SAE 1141 steel after reheated to 1218 °C. F: ferrite; P: pearlite; B: bainite; M: martensite. 16

2. The CCT diagram of the microalloyed SAE 1141 steel after reheated to 1218 °C and compressed 50% at 900 °C. F: ferrite; P: pearlite; B: bainite; M: martensite. 17

3. The CCT diagram of the microalloyed SAE 1141 steel after reheated to 1218 °C and compressed 50% at 1000 °C. F: ferrite; P: pearlite; B: bainite; M: martensite. 18

4. The CCT diagram of the microalloyed SAE 1141 steel after reheated to 1218 °C and compressed 50% at 1100 °C. F: ferrite; P: pearlite; B: bainite; M: martensite. 19

5. Strain distribution along AA' of a deformed specimen with a 50% height reduction. The original height of the specimen was 18 mm. There is small or no strains near the top (A) and bottom (A') surfaces. The strains are higher at locations close to the middle (O). The strain is small near the point D. The strain is calculated using the grain height measurements explained in figure 6. 20

6. The microstructural technique used to estimate the strain distribution after a cylindrical specimen was compressed. The technique is applicable only if the deformation is carried out at temperatures where no grain recrystallization takes place. 20

7. Picture of a production yoke. 21

8. Microstructure of a yoke (MA SAE 1141 steel) produced with a production schedule. 21

9. Microstructure of a laboratory specimen (d0 condition) cooled at a comparable rate of a production yoke. The ASTM austenite grain size number is 3.5. 22

10. Microstructure of a laboratory specimen (d0 condition) with a cooling time of 45.9 s to cool from 800 to 500 °C. 22

11. Microstructure of a laboratory specimen (d0 condition) with a cooling time of 24.8 s to cool from 800 to 500 °C. 23

12. Microstructure of a laboratory specimen (d0 condition) with a cooling time of 15.9 s to cool from 800 to 500 °C. 23

13. Microstructure of a laboratory specimen (d0 condition) with a cooling time of 12.3 s to cool from 800 to 500 °C. 24

14. Microstructure of a laboratory specimen (d2 condition) with a cooling time of 170.8 s to cool from 800 to 500 °C. The ASTM austenite grain size number is 6. 25

15. Microstructure of a laboratory specimen (d3 condition) with a cooling time of 129.2 s to cool from 800 to 500 °C. The ASTM austenite grain size number is 5.5. 25

16. Microstructure of a laboratory specimen after compressed 50% at 900 °C. The cooling time from 800 to 500 °C is 14.6 s. The banded structure is a result of transformation from flattened nonrecrystallized austenite grains. 26

17. Microstructure of a laboratory specimen after compressed 50% at 900 °C. The cooling time from 800 to 500 °C is 189 s. The prior austenite grain boundaries were not well outlined because ferrite nucleated not only along the prior austenite grain boundaries but also within austenite grains. 26

18. The true stress-true strain curve of the microalloyed SAE 1141 steel tested at 900 °C with a strain rate of 10 s^{-1}. 27

19. The true stress-true strain curve of the microalloyed SAE 1141 steel tested at 1000 °C with a strain rate of 10 s^{-1}. 28

20. The true stress-true strain curve of the microalloyed SAE 1141 steel tested at 1100 °C with a strain rate of 10 s^{-1}. 29

21. Log (stress)-vs.-log (strain) curves for tests at different temperatures. 30

CONTINUOUS-COOLING TRANSFORMATION CHARACTERISTICS AND HIGH-TEMPERATURE FLOW BEHAVIOR OF A MICROALLOYED SAE 1141 STEEL

Yi-Wen Cheng
Avinoam Tomer*

Materials Reliability Division
National Institute of Standards and Technology
Boulder, Colorado 80303-3328

This report presents the results of a thermomechanical processing (TMP) study on a microalloyed SAE 1141 forging steel. The primary objective of the study is to investigate the effects of deformation temperature on the phase-transformation kinetics and to determine the high-temperature flow characteristics of the steel. One-hit compression tests at a constant true strain rate of 10 s^{-1} were performed with a TMP simulator. Tests were performed at 900, 1000, and 1100 °C.

The results show that flow stress increased with decreasing temperature. In the strain range 0.35 to 0.6, the effect of temperature on the flow stress can be described by the equation, σ (MPa) = 2.93 exp[4944/T (K)]. Continuous-cooling transformation (CCT) diagrams determined following deformation at 1000 and 1100 °C were similar. However, deformation at 900 °C shifted the ferrite-plus-pearlite nose to a shorter time and produced a much finer ferrite-plus-pearlite microstructure. This is because the steel does not recrystallize at 900 °C after deformation imposed in this study. The usefulness of the CCT diagram and the relationship between deformation and austenite recrystallization are discussed.

Key words: continuous-cooling transformation; flow stress; forging steels; microalloyed steels; recrystallization; thermomechanical processing; true stress-true strain curves.

---

* Guest researcher, on leave from Nuclear Research Center-Negev, Beer Sheva, Israel.

I. INTRODUCTION

Microalloyed (MA) medium-carbon forging steels have been introduced to the automobile industry as economical substitutions for some quenched-and-tempered (Q-T) grades. Cost reduction is the driving force for developing MA steels, which are to be used in the as-cooled condition. Cost reduction is realized through the elimination of heat treatment, straightening, stress relieving, and improved machinability. MA steels can achieve tensile strengths comparable to those of Q-T steels, but with inferior impact properties. Research to improve the impact properties of the directly cooled MA steels is increasing. Several approaches to raising the toughness while lowering the ductile-to-brittle transition temperature have been cited in the literature [1-3]. These include: (1) lowering the carbon content from 0.5% to 0.35 or 0.25%; (2) lowering the reheating temperature and the finish-forging temperature to control the austenite (γ) grain size; (3) adding Ti (to produce TiN particles) to control γ grain size; (4) modifying the steel chemistry, such as increasing Mn or Si content; (5) controlling MnS inclusions to increase intragranular ferrite nucleation; and (6) producing low-carbon bainitic steels.

Lowering the deformation (finish-forging) temperature will change the γ grain morphology, which will, in turn, influence the austenite-to-ferrite transformation kinetics and the final microstructure. Lowering the deformation temperature will also increase the flow resistance of the steel and reduce the forgeability. The goal of the present study is to investigate the effects of deformation temperature on the transformation kinetics of a MA SAE 1141 steel in terms of continuous-cooling transformation (CCT) diagrams, and to determine the high-temperature flow characteristics of the steel. Attempts were also made to generalize the effects of deformation temperature on flow stress, and the recrystallization of γ after deformation.

II. EXPERIMENTAL PROCEDURES

The material used in this study is a MA SAE 1141 steel, which was continuously cast and rolled into 25.4 mm round bars. The steel was received in the as-rolled condition. The chemical composition of the steel in mass percent is given in table 1. Cylindrical specimens, 9 mm in diameter by 18 mm in height, were taken from the bars. Specimens were reheated to 1218 °C with an induction heater at a rate of 1 °C s^{-1} and soaked for 5 min. One series of specimens was cooled directly from 1218 °C with forced helium gas to ambient temperature at different rates to establish a continuous-cooling transformation (CCT) diagram.

To investigate the effects of deformation on the CCT characteristics and to determine the flow behavior at different temperatures, three series of specimens were treated with the above mentioned reheating and soaking conditions and then cooled at a rate of 1 °C s^{-1} to three different deformation temperatures: 900, 1000, and 1100 °C (with one series of specimens at each temperature). The specimens were compressed 50% in height at the deformation temperatures with a constant true strain rate of 10 s^{-1}. Following the compression, the specimens were cooled immediately to ambient temperature at different rates to establish CCT diagrams. The experiments were performed with a hot-deformation apparatus, described in a previous report [4]. The detailed procedures to determine the austenite-to-ferrite (or other transformation products) transformation temperatures and the true stress-true strain curves were previously described [5].

Table 1. Chemical composition of microalloyed SAE 1141 steel (mass percent).

C	Mn	P	S	Si	Cu	Ni	Cr	Mo	Nb	Sn
0.42	1.49	0.015	0.099	0.26	0.16	0.06	0.06	0.009	0.039	0.006

Following the thermomechanical (TMP) treatments, all specimens were examined with a light microscope to study the microstructures. Macro- and microhardness testers were also used to characterize the specimens.

III. EXPERIMENTAL RESULTS AND DISCUSSION

Continuous-Cooling Transformation (CCT) Characteristics

A CCT diagram of a steel reveals, in a time-temperature space, the phase transformations that take place during continuous cooling at different cooling rates. The diagram can be used to estimate the hardenability of a steel and to predict the room-temperature microstructure and its related properties, such as tensile strength, hardness, machinability, and fatigue strength. However, the CCT diagram of a steel is not unique. Its relative position and shape in the time-temperature space are influenced by the γ condition prior to transformation, such as grain size, the state of alloying elements (dissolved in γ or precipitated as compounds), and the state of γ (fully recrystallized or deformed).

Figures 1 through 4 present the CCT diagrams of the MA SAE 1141 steel with the experimental conditions described in table 2. The Ac_3 temperature of 789 °C shown on the figures was calculated using equation (1),

$$Ac_3\ (°C) = 910 - 203C - 15.2Ni + 44.7Si + 104V + 31.5Mo + 13.1W. \qquad (1)$$

Table 2. Experimental conditions.

Condition	Deformation Temperature, °C
d0	No Deformation
d1	900
d2	1000
d3	1100

Also shown on the CCT diagrams are the progression of transformation from γ to the product phases and the Rockwell C (R_c) hardness numbers of specimens cooled with different rates. The percentages shown on the figures indicate the volume fraction of γ that has transformed to the product phases. For instance, 10% means that 10% of γ has transformed to the product phases such as ferrite plus pearlite (F + P), and the remainder, 90%, is still γ. Based on the information on progression of transformation, we can estimate the volume fraction of each individual microconstituent at room temperature. Thus, room-temperature mechanical properties can be estimated.

With reheating and no deformation (condition d0), the tip of (F + P) nose is at 20 s. With deformation, the (F + P) nose shifts to a shorter time. This is attributed to smaller effective γ grains prior to transformation. The small effective γ grains can be either physically small grains after recrystallization or heavily deformed grains without recrystallization. In the present study, conditions d2 and d3 are physically small and condition d1 is heavily deformed. As shown in figure 2, the heavily deformed grains are very effective in enhancing the nucleation of ferrite. This results in not only shifting the (F + P) nose to a much shorter time (8 s in condition d1), but producing a finer ferrite-plus-pearlite structure (figure 17). The heavily deformed γ grains provide ferrite-nucleation sites not only along the grain boundaries but also at areas of high stored energy such as substructures and dislocation bands.

In addition to enhancing the (F + P) formation, deformation at 1000 and 1100 °C (conditions d2 and d3) seems to promote the formation of upper bainite at slow cooling rates (figures 3 and 4). The reason for this effect is not clear at the present. The formation of upper bainite will result in lower toughness and higher strength [7,8].

When interpreting the phase-transformation temperatures shown by the CCT diagrams, the effects of nonuniform cooling within the specimen have to be considered. The specimens used for the present experiments were cylinders 9 mm in diameter by 18 mm in height. Nonuniform temperature distribution within a specimen is expected during cooling,

especially in cases of rapid cooling with forced gas. The exact temperature distribution within a specimen under different cooling conditions has not been characterized and the temperature was measured at the peripheral mid-height of the cylinder. The temperature at the central portion inside the cylinder is expected to be higher than that measured at the surface. This has to be taken into consideration when one interprets the phase-transformation temperatures. For a slow cooling, nevertheless, the measured ferrite-start temperature at 630 °C of this study is in good agreement with the calculated temperature of 638 °C* [9]. In addition to temperature inhomogeneity, there are segregation and nonuniform strain distribution during and after deformation in a specimen, as shown in figure 5. The inhomogeneities in temperature, chemistry, and strain distribution will influence the transformation kinetics.

The intended application of the MA 1141 steel is in the directly cooled condition. Thus, the CCT diagrams presented in figures 1 through 4 are directly applicable to production conditions, providing the thermal and the deformation histories are similar, that is, similar γ conditions prior to phase transformation. For example, the thermal profile of a fan-cooled forged yoke (figure 7) shown as the dashed line in figure 1 [10] is comparable to that shown in the far-right curve. The microstructures, as shown in figures 8 and 9, of the yoke (finish-forging temperature was about 1218 °C) and a laboratory specimen with a comparable cooling profile are similar. The average R_c hardness is approximately 20 for both the yoke section and the laboratory specimen.

Metallography

Unless specified, microstructures were taken at locations away from free surfaces, so that they represent the bulk property. In the case of laboratory specimens, the locations are close to point O in figure 5. The specimens were etched with either 2% nital or Vilellas' reagent.

---

*The temperature was calculated using the formula: 878 - 295C - 78Mn (2)

Figure 8 represents the microstructure of a forged yoke produced in a production plant: it was fan cooled after forging. The predominant microconstituent is pearlite plus ferrite. Ferrite appears in the allotriomorphic form along the prior γ grain boundaries and in the form of Widmanstätten plates across the prior γ grains. As shown in figure 9, a similar microstructure has been reproduced in a laboratory specimen that received a comparable thermal treatment. With increases in cooling rate, the microstructure changes, which are shown in figures 10 through 13 and are described as follows. The rate of cooling is reported in terms of the time, denoted as Δt, to cool from 800 to 500 °C.

Figure 9: Δt is 159.0 s and the microstructure is predominantly massive pearlite, which appears as dark areas. The allotriomorphic α forms along the prior γ grain boundaries and the Widmanstätten α forms across the grains.

Figure 10: Δt is 45.9 s. The volume fraction of the allotriomorphic α diminishes and the microstructure is predominantly fine Widmanstätten α (needle-like white areas) plus pearlite (dark areas).

Figure 11: Δt is 24.8 s. The microstructure consists of a mixture of fine Widmanstätten α, pearlite, bainite, and martensite. With a light microscope, it is difficult to differentiate between Widmanstätten α plus pearlite and bainite. Bulky white areas that appear away from prior γ grain boundaries, are usually martensite.

Figure 12: Δt is 15.9 s. The Widmanstätten α plus pearlite disappears, and the microstructure consists of bainite and martensite. The bainite mainly forms along the prior γ grain boundaries and appears in dark in these micrographs.

Figure 13: Δt is 12.3 s. The predominant microconstituent is martensite with a small amount of bainite present.

After deformation at 1000 (d2 condition) and 1100 °C (d3 condition), the γ grains recrystallized. No pancaked grains were observed. The effect of deformation at these two temperatures is the decrease in recrystallized γ grain size. This effect is evident by comparing figures 9, 14, and 15. The γ grain-size numbers for specimens with treatments of d0, d2, and d3 were determined to be 3.5,6, and 5.5 using the comparison procedure [11]. The corresponding equivalent grain diameters are 121, 60, and 51 μm, respectively. The more Widmanstätten α shown in figure 15 is attributed to a higher cooling rate in this specimen. Δt is 129.2 s for this specimen, 159.0 s in specimen shown in figure 9 and 170.8 s for that shown in figure 14.

The observed grain diameters are consistent with the theoretical predictions. Assuming only static recrystallization takes place (no dynamic recrystallization), which is reasonable for the present testing conditions, the recrystallized grain diameter can be calculated using equation [12],

$$d_{rex} = D\, d_o^{0.67}\, \epsilon^{-0.67}, \qquad (3)$$

where d_{rex} is the recrystallized grain diameter, d_o is the grain diameter before deformation, ϵ is the total true strain, and D is a constant. Deformation temperature has little or no effect on d_{rex} [12,13]. Grain growth after completion of static recrystallization is negligible for Nb-treated steels with deformation temperatures below 1200 °C [12]. Using values of d_o = 121 μm, ϵ = 0.69 (50% thickness reduction), and d_{rex} = 51 and 60 μm, we obtained values of D = 1.60 and 1.88 $\mu m^{0.33}$. These calculated values of D are in good agreement with those reported in the literature [12].

Deformation at 900 °C (condition d1) flattened the γ grains, which are shown in figure 16. The banded darker areas around the prior γ grain boundaries are a mixture of polygonal ferrite and bainite. The large lighter areas are martensite. No recrystallized γ grains were observed. The microstructure shown in figure 16 was obtained with a specimen that was rapidly cooled after deformation. The cooling time from 800 to 500 °C was 14.6

s. With a cooling time from 800 to 500 °C equal 189 s, ferrite nucleated along prior γ grain boundaries as well as within the grains. As shown in figure 17, this results in less well defined prior γ grain boundaries than those shown in figure 9. The continuous ferrite grains and the size of pearlite colonies in figure 17 are much smaller than those in figures 8 and 9. This type of microstructure is desirable because it improves toughness and strength simultaneously. We conclude from the metallographic examination that the nonrecrystallization temperature for the MA SAE 1141 steel is between 900 and 1000 °C under the present testing condition.

Hardness Measurements

Both the R_c hardness and the Vickers microhardness were measured on selected specimens after different TMP treatments. The results of R_c-hardness measurements are reported in figures 1 through 4 in the CCT diagrams. After a cooling equivalent to that in still air, the specimens have R_c-hardness numbers ranging from 20 to 22 for all the specimens tested. The hardness number increases with increasing cooling rate. The microhardness measurements were conducted with a load of 490 N. The microhardness numbers (DPH) correspond to individual microconstituents are presented in table 3.

True Stress-vs.-True Strain Curves

The true stress-vs.-true strain curves are shown in figures 18, 19, and 20 for tests at 900, 1000, and 1100 °C, respectively. The curves show no occurrence of dynamic recrystallization during the tests at any of the testing temperatures. Occurrences of dynamic

Table 3. Results of microhardness measurements.

Ferrite	Pearlite	Bainite	Martensite
198	203	258-297	396-444

recrystallization will show a decrease of stress with increasing strain. The drop in stress close to the end of each test, as shown in figures 18 through 20, is an inherent deficiency of the mechanical testing machine. It should not be considered as indications of dynamic recrystallization. As shown in the figures, the stress at a given strain decreases with increasing temperature.

Without structural changes such as precipitation, strain aging, or recrystallization, the temperature dependence of flow stress at constant strain and strain rate can be represented by [14]

$$\sigma = C \exp[Q/(RT)], \tag{4}$$

where σ = flow stress, MPa,
Q = an activation energy for plastic flow, kJ/mol,
R = universal gas constant, 8.314 J/(mol K),
T = testing temperature, K, and
C = a constant.

Using the values given in table 4, we obtain Q and C equal to 41.1 kJ/mol and 2.93 MPa, respectively. At a strain rate of 10 s^{-1}, equation (5) is adequate to predict the flow stress in the strain range 0.35 to 0.6,

$$\sigma = 2.93 \exp(4944/T). \tag{5}$$

Table 4. Values used to calculate Q and C in equation (4).

T (K)	σ (MPa)*	$(1/T)\times10^3$	$\ell n\ \sigma$
1173	196.5	0.853	5.28
1273	146.5	0.786	4.99
1373	106.0	0.728	4.66

* values obtained from figures 18 through 20 at a strain level equal to 0.4.

In figure 21, (log σ) is plotted vs. (log ϵ) for tests at different temperatures. ϵ is the true strain. Evidently, d(log σ)/d(log ϵ) is not constant. It decreases with increasing strain. This indicates that the σ-ϵ behavior does not conform to the simple power-curve relation, $\sigma = K\epsilon^n$. The slope of (log σ) vs. (log ϵ), as shown in figure 21, ranges from 0.15 to 0.25.

Using Recrystallization to Control Austenite Grain Size

Equation (3) can be used to estimate the recrystallized γ grain size after deformation. It can also be used to design a workable deformation schedule for achieving the optimal γ grain refinement. Of course this has to take into consideration factors such as machine capacity and product shape control. Austenite grain refinement through recrystallization can be illustrated with the following example: Calculations were made to predict the final γ grain sizes after four different deformation schedules. The calculations were performed with the following conditions:

a. The workpiece is a flat product with an initial thickness of 2.5 cm.

b. The workpiece is compressed to a final thickness of 1 cm with four different deformation schedules.

c. Deformations are performed so that the static recrystallization has completed between deformations. No grain growth occurs after recrystallization. No deformation is performed at temperatures below T_{nr}.

d. The values of D and d_o in equation (3) are 1.60 and 121, respectively.

The results are presented in table 5. A close examination of table 5 gives the following conclusions:

a. With the same initial and final dimensions, the least number of hits produces the smallest austenite grain size (series 1).

b. With the same number of hits, the austenite grain size can be refined with an optimum deformation schedule. For example, series 4 produced a smaller

Table 5. Computed austenite grain sizes after different deformation schedules.

	After Hit(s)	Thickness, cm	d_{rex}, μm
Series 1		0.25000E+01	0.12100E+03
	1	0.15000E+01	0.62380E+02
	2	0.10000E+01	0.46717E+02
Series 2		0.25000E+01	0.12100E+03
	1	0.20000E+01	0.10865E+03
	2	0.15000E+01	0.85269E+02
	3	0.10000E+01	0.57600E+02
Series 3		0.25000E+01	0.12100E+03
	1	0.20000E+01	0.10865E+03
	2	0.15000E+01	0.85269E+02
	3	0.12500E+01	0.98399E+02
	4	0.10000E+01	0.94596E+02
Series 4		0.25000E+01	0.12100E+03
	1	0.22000E+01	0.15781E+03
	2	0.17500E+01	0.12764E+03
	3	0.15000E+01	0.14428E+03
	4	0.10000E+01	0.81933E+02

recrystallized γ grain than series 3. Note that series 4 is not an optimum schedule, which can be obtained through careful trial-and-error simulations.

IV. SUMMARIES AND CONCLUDING REMARKS

The main objectives of the study include:

1. investigating the effects of finish-forging temperature on the continuous-cooling transformation (CCT) characteristics and the final microstructure of the microalloyed SAE 1141 steel, and

2. determining the flow behavior of the steel at high temperature under high strain rate.

True stress-vs.-true strain curves were obtained at 900, 1000, and 1100 °C with a constant true strain rate of 10 s^{-1}. Flow stress increases with decreasing temperature. In the strain range 0.35 to 0.6, the effect of temperature on the flow stress can be described by the equation,

$$\sigma = 2.93 \exp(4944/T) \quad (5)$$

where σ is flow stress in MPa and T is temperature in K.

The main factors that influence the CCT characteristics are the type and amount of alloying elements dissolved in austenite and the austenite grain size before transformation. For the microalloyed SAE 1141 steel, deformation (forging) temperature has only a slight effect on the recrystallized austenite grain size after deformation if the temperature is above the nonrecrystallization temperature, T_{nr}, and below 1200 °C. Based on the results obtained in the present study, T_{nr} of the steel is between 900 and 1000 °C. The most prevailing factor in determining the recrystallized grain size is the strain of each deformation. The present study shows that there is no observed difference in CCT characteristics between 50% thickness reduction at 1000 °C and at 1100 °C. Therefore, the microstructures at room temperature are similar in both cases.

Deformation below T_{nr}, such as at 900 °C, flattens the austenite grains and produces high dislocation density and substructures inside the austenite grains. These promote ferrite formation. Ferrite then forms at a shorter time during continuous cooling below Ar_3 temperature, and ferrite grains are small. This is a desirable microstructure because it offers an excellent combination of strength and toughness. However, flow resistance of the steel is relatively high at temperatures below T_{nr}. Therefore, this practice might not be practical for most of the forging applications.

A small ferrite grain size at room temperature can also be achieved by austenite grain refinement through recrystallization. By proper design of the deformation schedule using

the equation, $d_{rex} = D\ d_o^{0.67}\ \epsilon^{-0.67}$, the recrystallized austenite grains can be minimized. In the above equation, d_{rex} is the recrystallized austenite grain diameter after each deformation, d_o is the austenite grain diameter before each deformation, ϵ is the true strain of each deformation, and D is a constant. The grain refinement through recrystallization seems to be suitable for forging applications.

CCT diagrams can be used to predict the room-temperature microstructure and its related properties. CCT diagrams can also be used as a guide to assess the cooling-rate sensitivity of properties. For instance, in the area close to the tip of the nose, a small change in cooling rate will have a large influence on the final microstructure and properties. To ensure uniform and consistent properties, we should avoid cooling of the steel at rates that will pass through the area close to the tip of the nose.

V. ACKNOWLEDGMENTS

This study was performed in collaboration with J. H. Hoffmann of Chrysler Motors Corporation and A. D. McCrindle of Stelco Fastener & Forging Company, who provided materials and helpful discussions during the course of the study. The assistance of C. L. Sargent in performing data reduction is acknowledged.

VI. REFERENCES

[1] M. Korchynsky and J. R. Paules, "Microalloyed Forging Steels - A State of the Art Review," Int'l Congress and Exposition, Feb. 27-Mar. 3, 1989, Detroit, MI, Paper No. 89081.

[2] T. Ouchi, T. Takahashi, and H. Takada, "Improvement of the Toughness of Hot Forged Products through Intragranular Ferrite Formation," Proc. of the 20th Mechanical Working and Steel Processing Conf., Oct. 23-26, 1988, Dearborn, MI, pp. 65-72.

[3] K. Matysumoto, et. al., "Development of Low-Carbon Bainitic Bar Steel for Hot Forged Use," ibid., pp. 73-81.

[4] Y. W. Cheng, Y. Rosenthal, and H. I. McHenry, "Development of a Computer-Controlled Hot-Deformation Apparatus at NIST," NISTIR 89-3925, National Institute of Standards and Technology, Boulder, CO (October, 1989).

[5] Y. W. Cheng and C. L. Sargent, "Data-Reduction and Analysis Procedures Used in NIST's Thermomechanical Processing Research," NISTIR 90-3950, National Institute of Standards and Technology, Boulder, CO (August, 1990).

[6] K. W. Andrews, "Empirical Formulae for the Calculation of Some Transformation Temperatures," JISI, Vol. 203 (July, 1965), pp. 721-727.

[7] K. J. Irvine, "A Comparison of the Bainite Transformation with Other Strengthening Mechanisms in High-Strength Structural Steel," Symposium: Strengthening Mechanisms in Steel, Climax Molybdenum Company, AMAX, Ann Arbor, MI (1969), pp. 55-65.

[8] The Making, Shaping and Treating of Steel, 9th edition, edited by H. E. McGannon, United States Steel, Pittsburgh, PA (1971), p. 1091.

[9] M. Atkins, Atlas of Continuous Cooling Transformation Diagrams for Engineering Steels, American Society for Metals, Metals Park, OH, 1980.

[10] J. H. Hoffmann, Chrysler Motors Corporation, Highland Park, MI, private communication.

[11] ASTM designation: E 112-88, Standard Test Methods for Determining Average Grain Size, in: Annual book of ASTM Standards, 1990.

[12] C. M. Sellars, "The Physical Metallurgy of Hot Working," in: Hot Working and Forming Processes, edited by C. M. Sellars and G. J. Davies, The Metals Society, London (1980), pp. 3-15.

[13] W. Roberts et al., "Prediction of Microstructure Development during Recrystallization Hot Rolling of Ti-V Steels," in: HSLA Steels - Technology & Applications, edited by M. Korchynsky, ASM, Metals Park, OH (1984), pp. 67-84.

[14] G. E. Dieter, Mechanical Metallurgy, second edition, McGraw-Hill Book Company, New York, 1976.

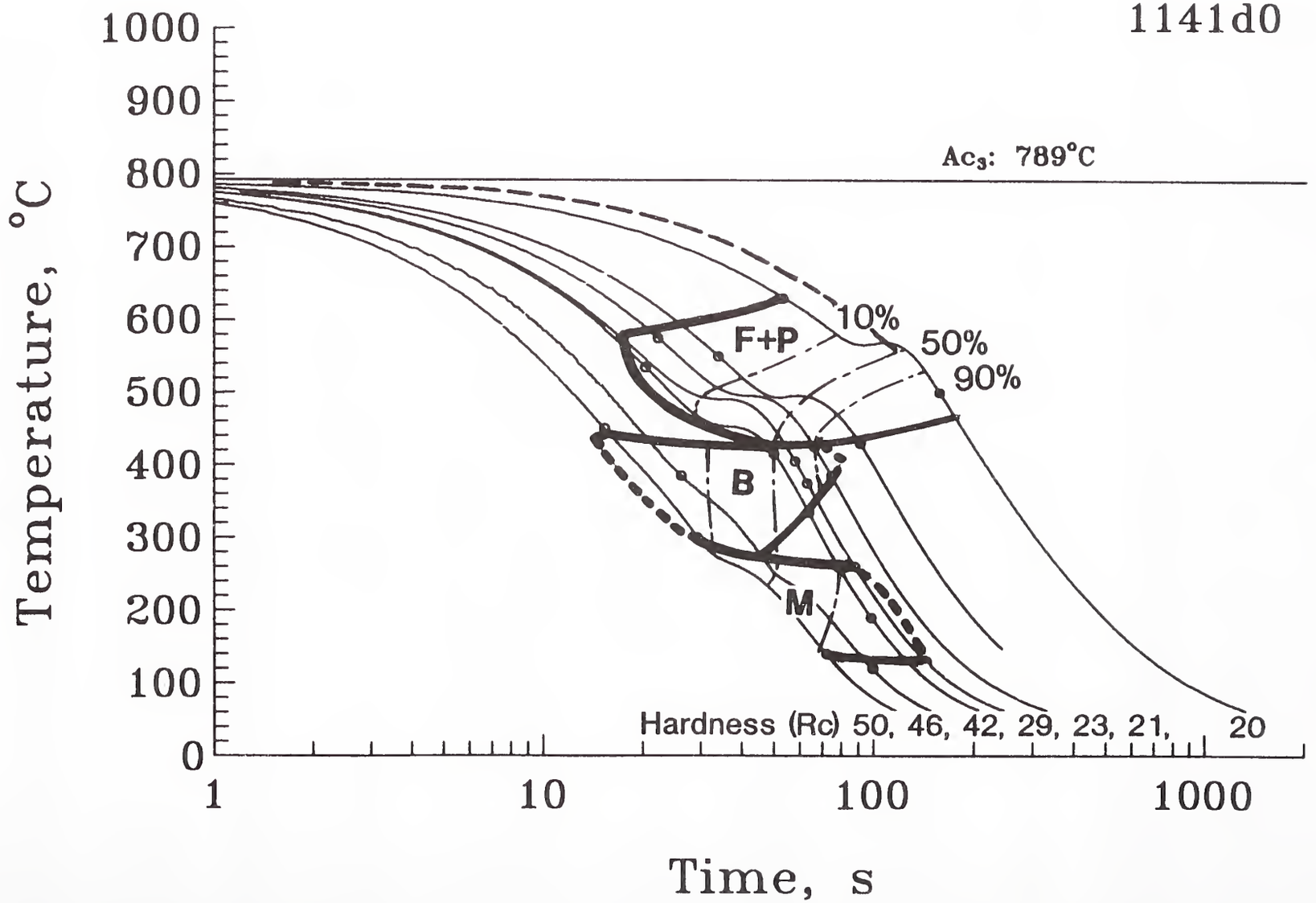

Figure 1. The CCT diagram of the microalloyed SAE 1141 steel after reheated to 1218°C. F: ferrite; P: pearlite; B: bainite; M: martensite.

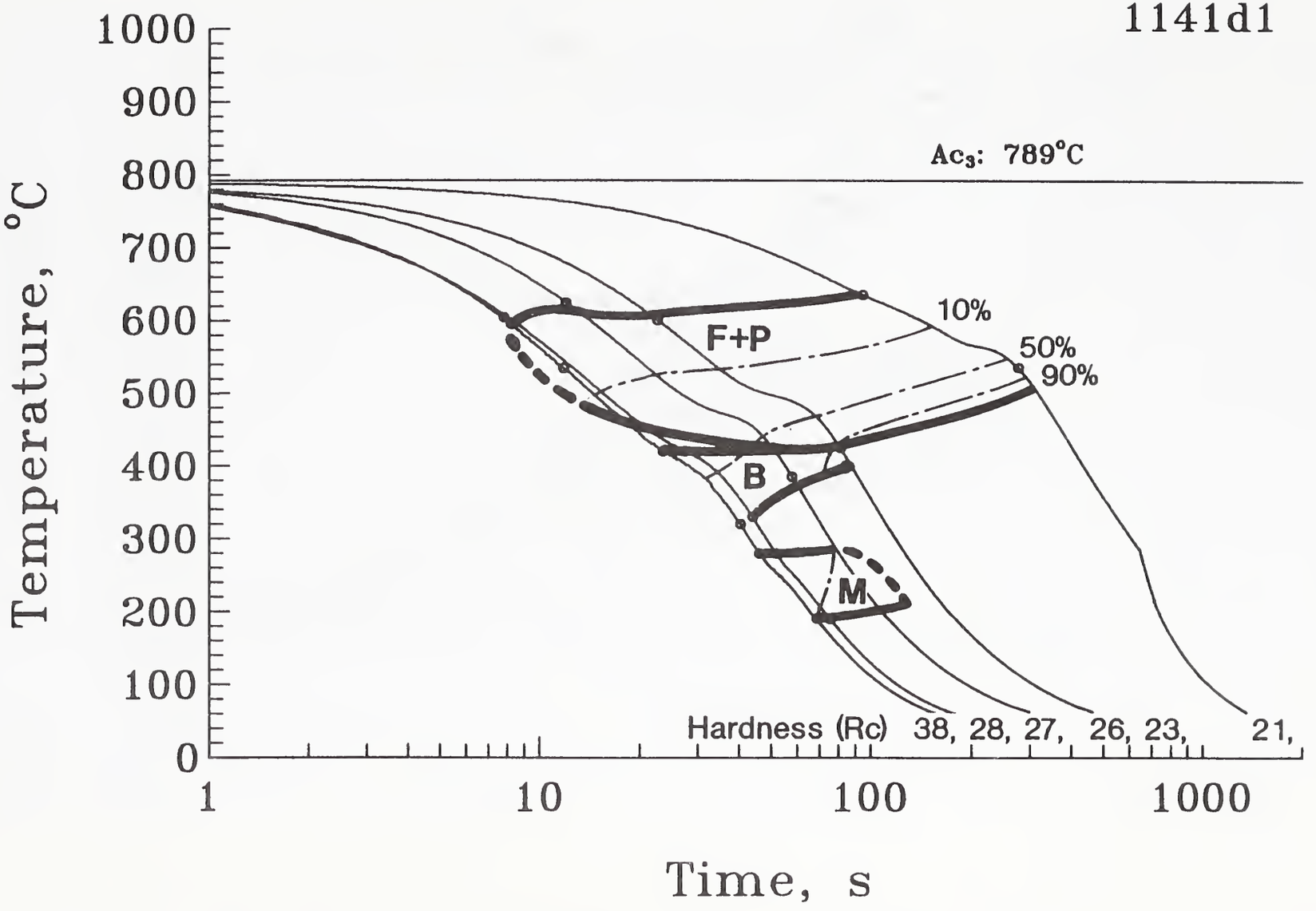

Figure 2. The CCT diagram of the microalloyed SAE 1141 steel after reheated to 1218°C and compressed 50% at 900°C. F: ferrite; P: pearlite; B: bainite; M: martensite.

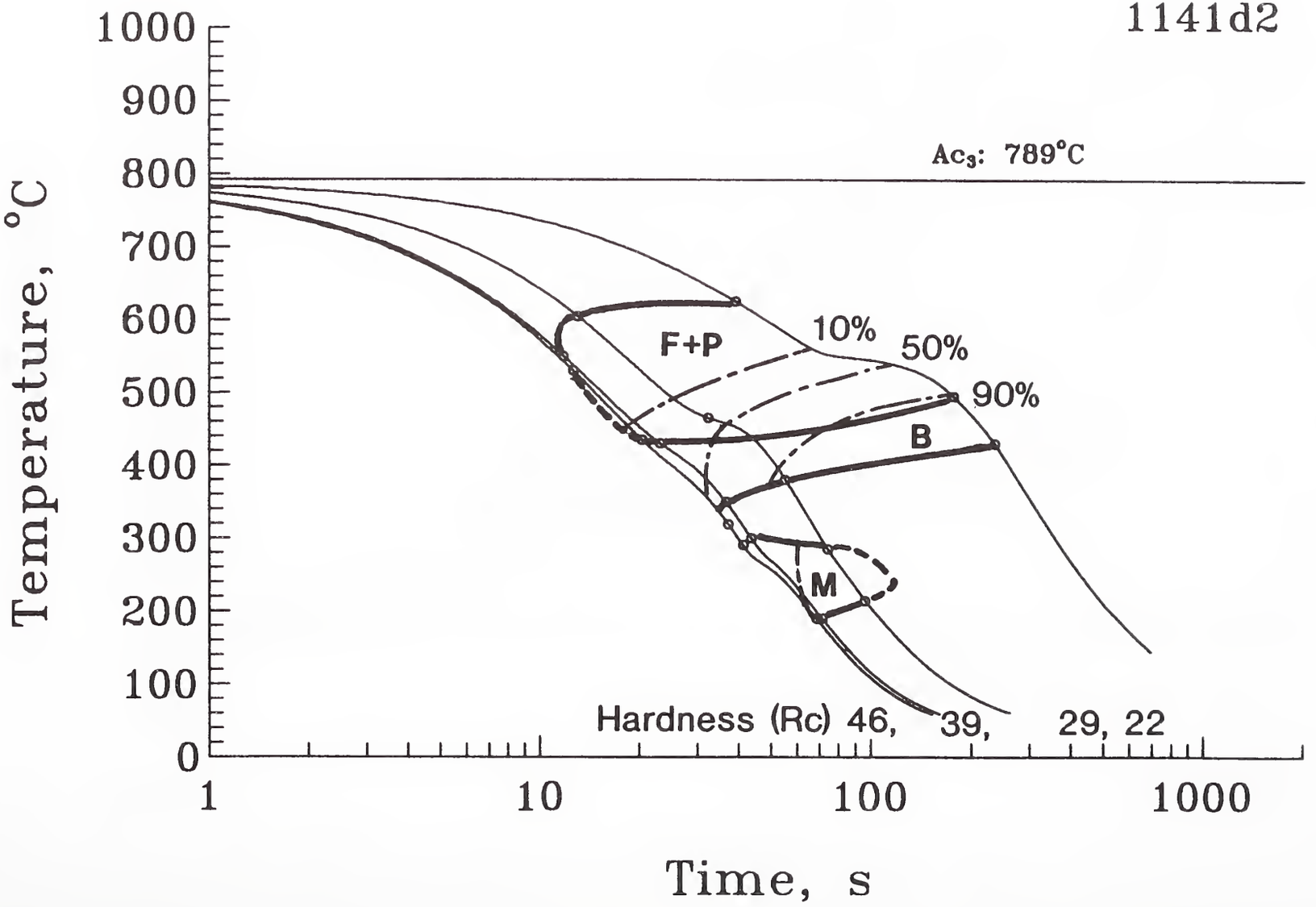

Figure 3. The CCT diagram of the microalloyed SAE 1141 steel after reheated to 1218°C and compressed 50% at 1000°C. F: ferrite; P: pearlite; B: bainite; M: martensite.

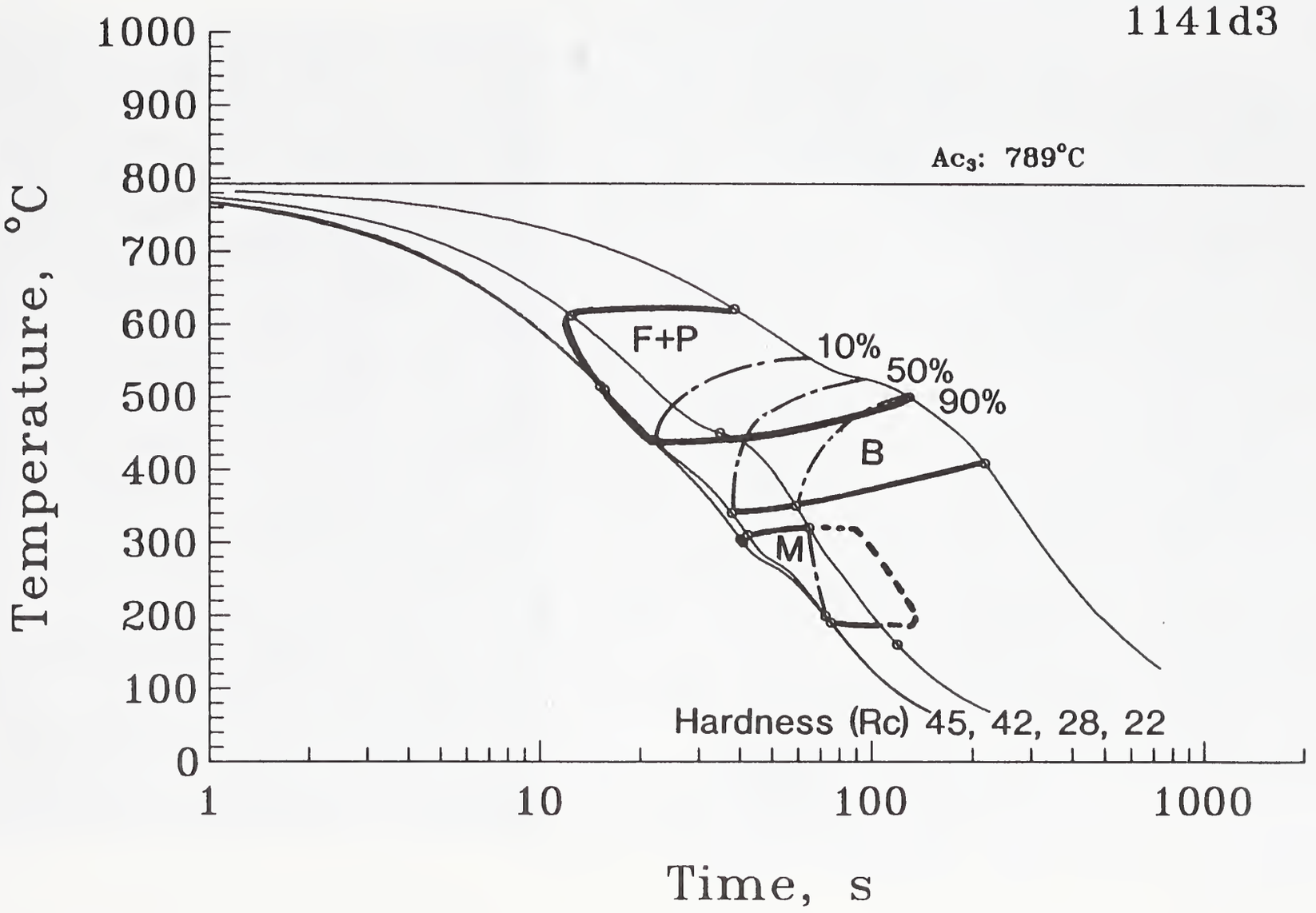

Figure 4. The CCT diagram of the microalloyed SAE 1141 steel after reheated to 1218°C and compressed 50% at 1100°C. F: ferrite; P: pearlite; B: bainite; M: martensite.

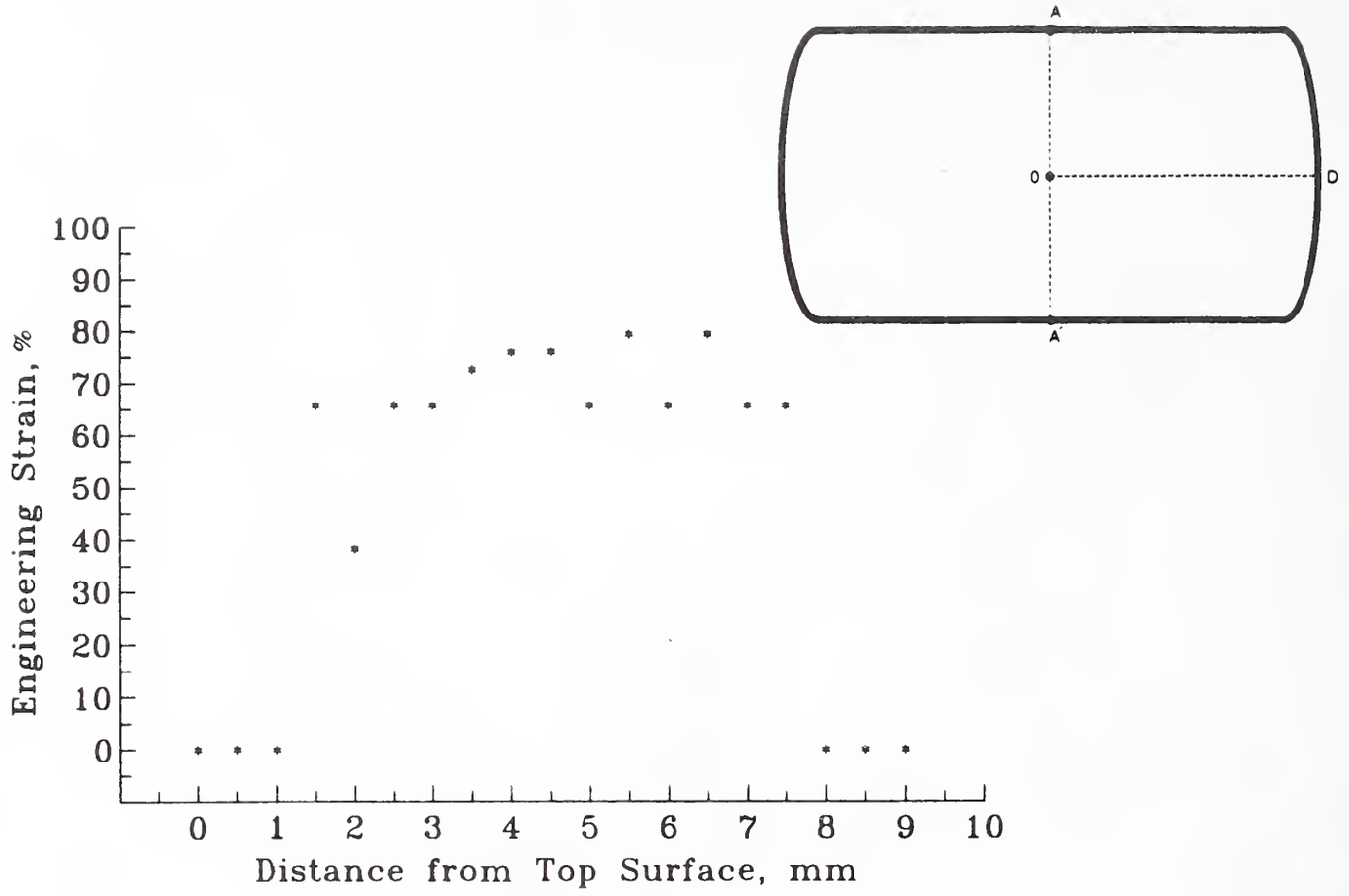

Figure 5. Strain distribution along AA' of a deformed specimen with a 50% height reduction. The original height of the specimen was 18 mm. There is small or no strain near the top (A) and bottom (A') surfaces. The strains are higher at locations close to the middle (O). The strain is small near the point D. The strain is calculated using the grain height measurements explained in figure 6.

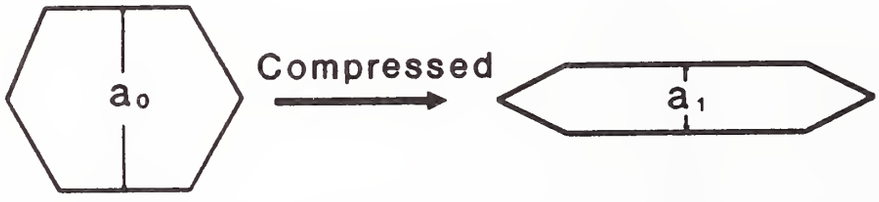

$$\text{Engineering Strain (\%)} = \frac{a_0 - a_1}{a_0} \times 100$$

Figure 6. The microstructural technique used to estimate the strain distribution after a cylindrical specimen was compressed. The technique is applicable only if the deformation is carried out at temperatures where no grain recrystallization takes place.

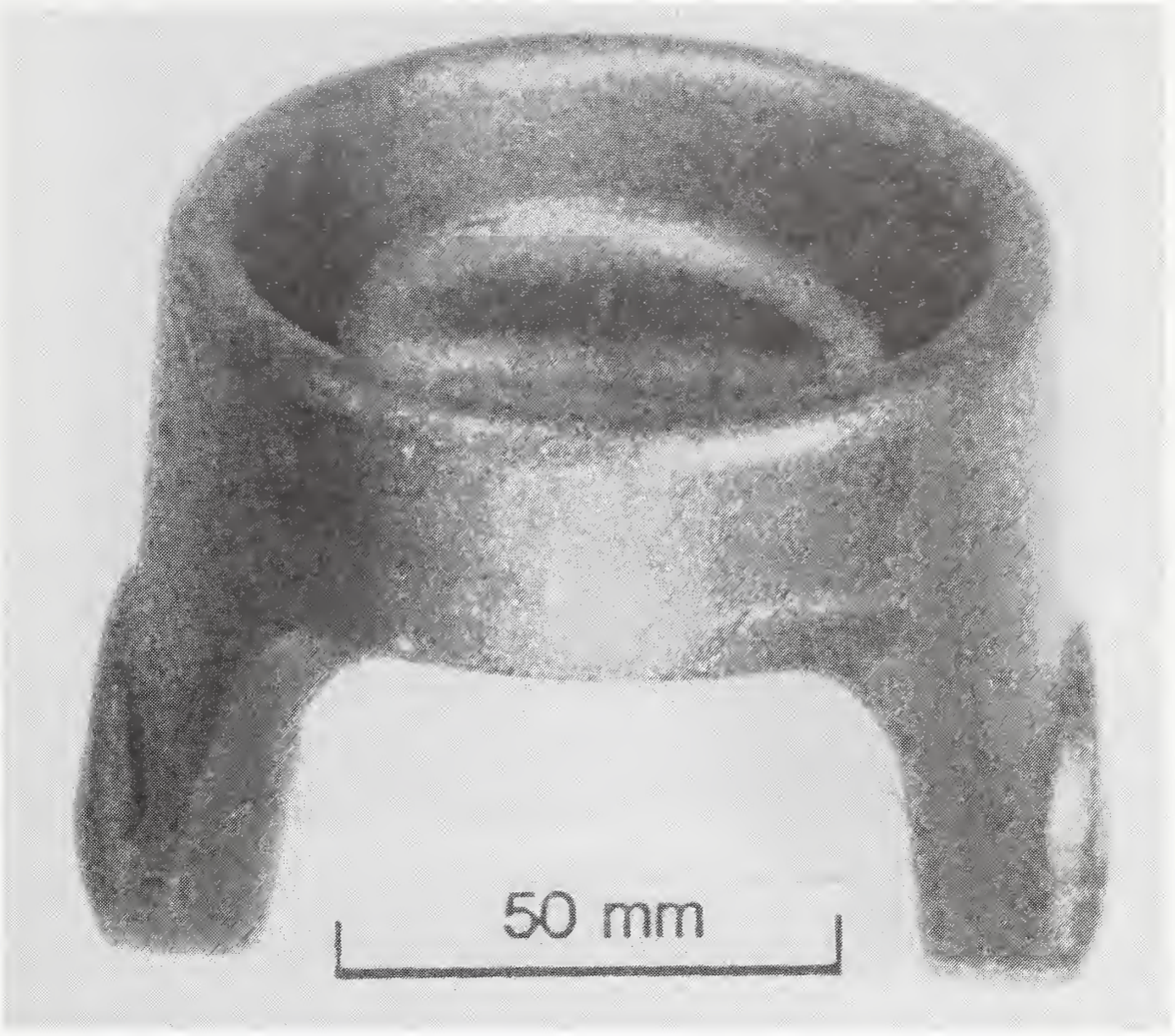

Figure 7. Picture of a production yoke.

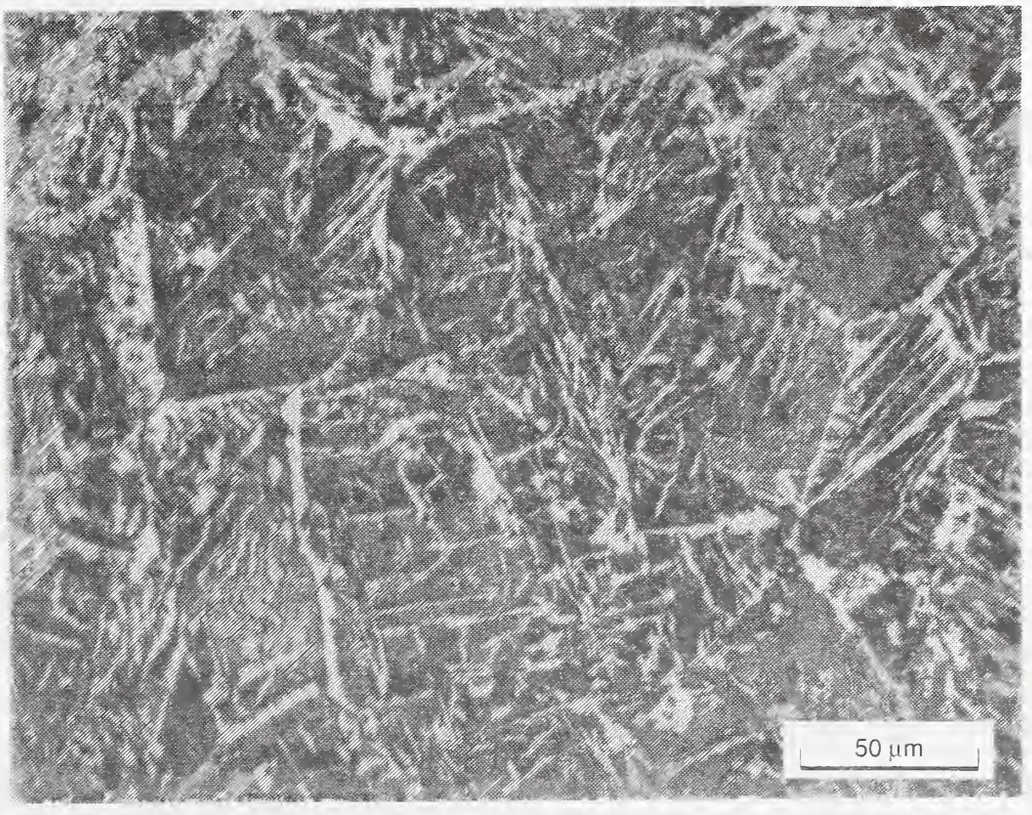

Figure 8. Microstructure of a yoke (MA SAE 1141 steel) produced with a production schedule.

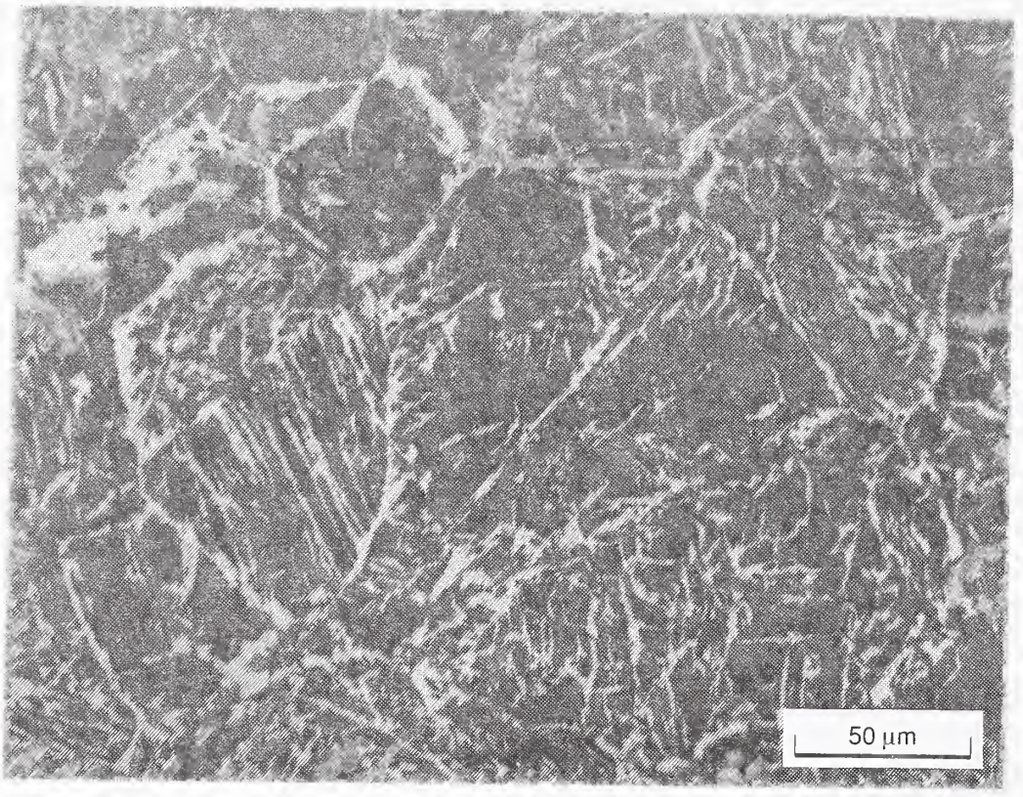

Figure 9. Microstructure of a laboratory specimen (d0 condition) cooled at a comparable rate of a production yoke. The ASTM austenite grain size number is 3.5.

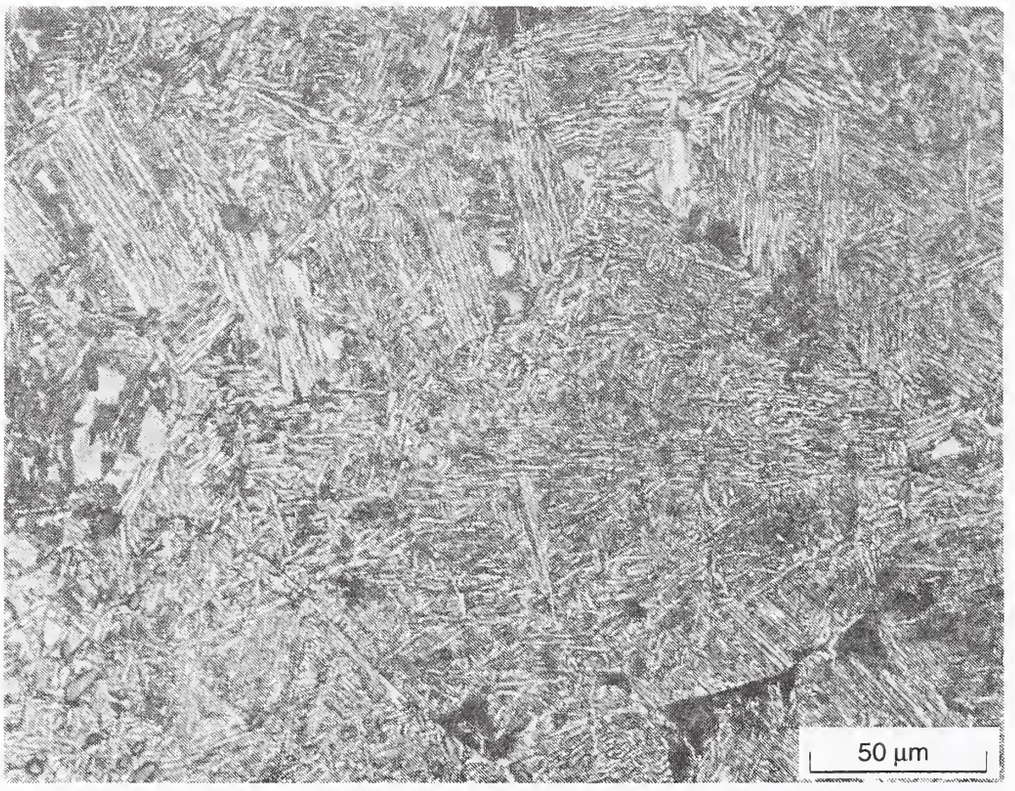

Figure 10. Microstructure of a laboratory specimen (d0 condition) with a cooling time of 45.9 s to cool from 800 to 500°C.

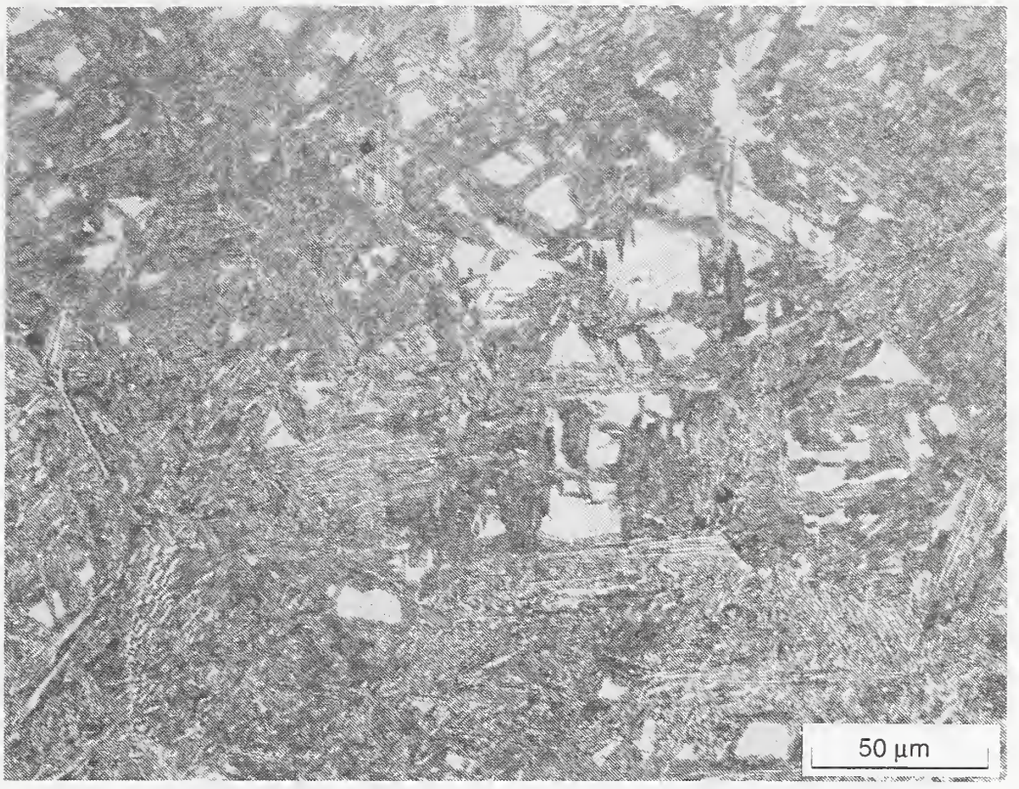

Figure 11. Microstructure of a laboratory specimen (d0 condition) with a cooling time of 24.8 s to cool from 800 to 500°C.

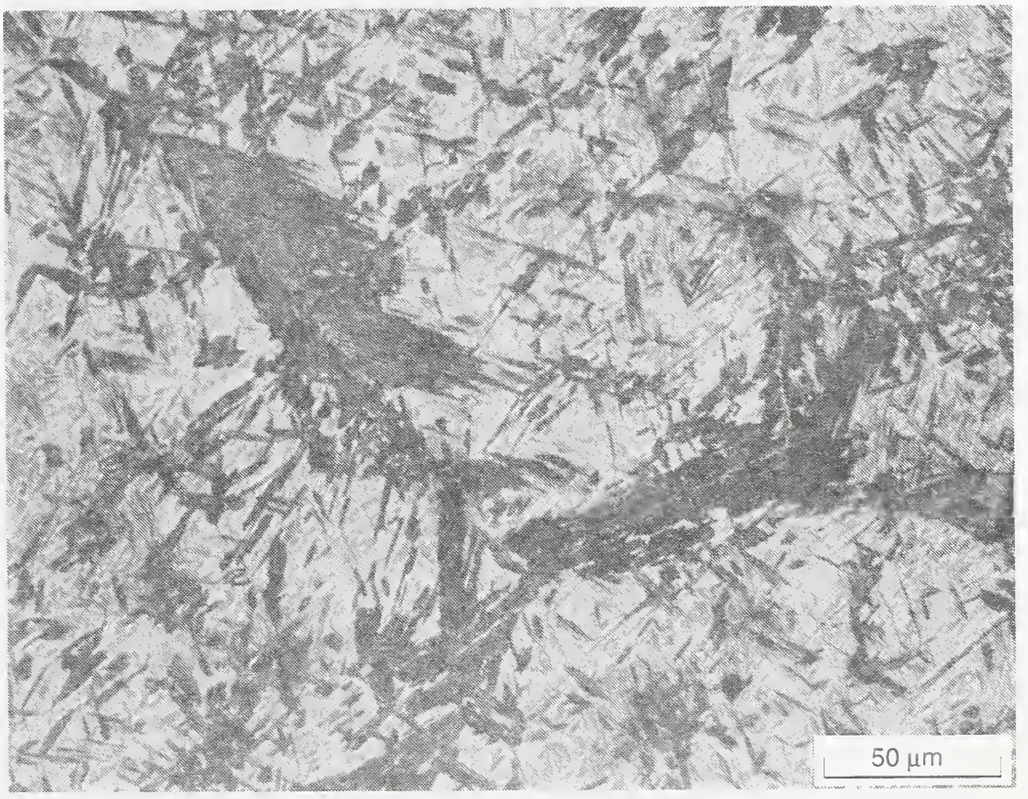

Figure 12. Microstructure of a laboratory specimen (d0 condition) with a cooling time of 15.9 s to cool from 800 to 500°C.

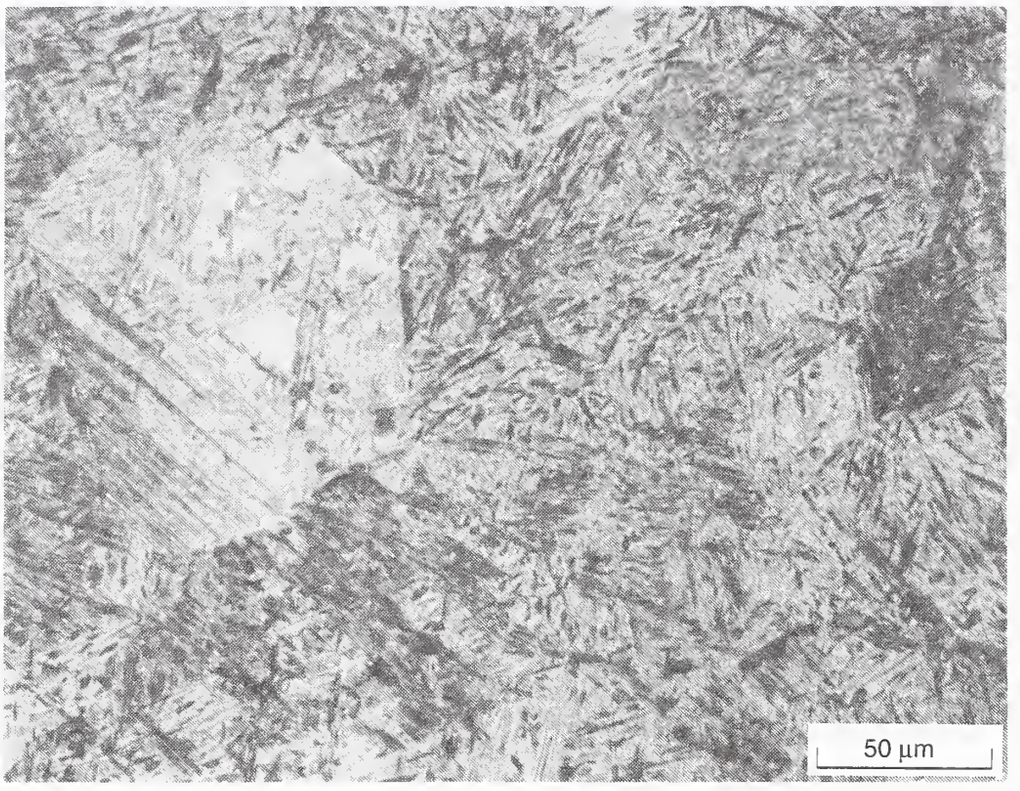

Figure 13. Microstructure of a laboratory specimen (d0 condition) with a cooling time of 12.3 s to cool from 800 to 500°C.

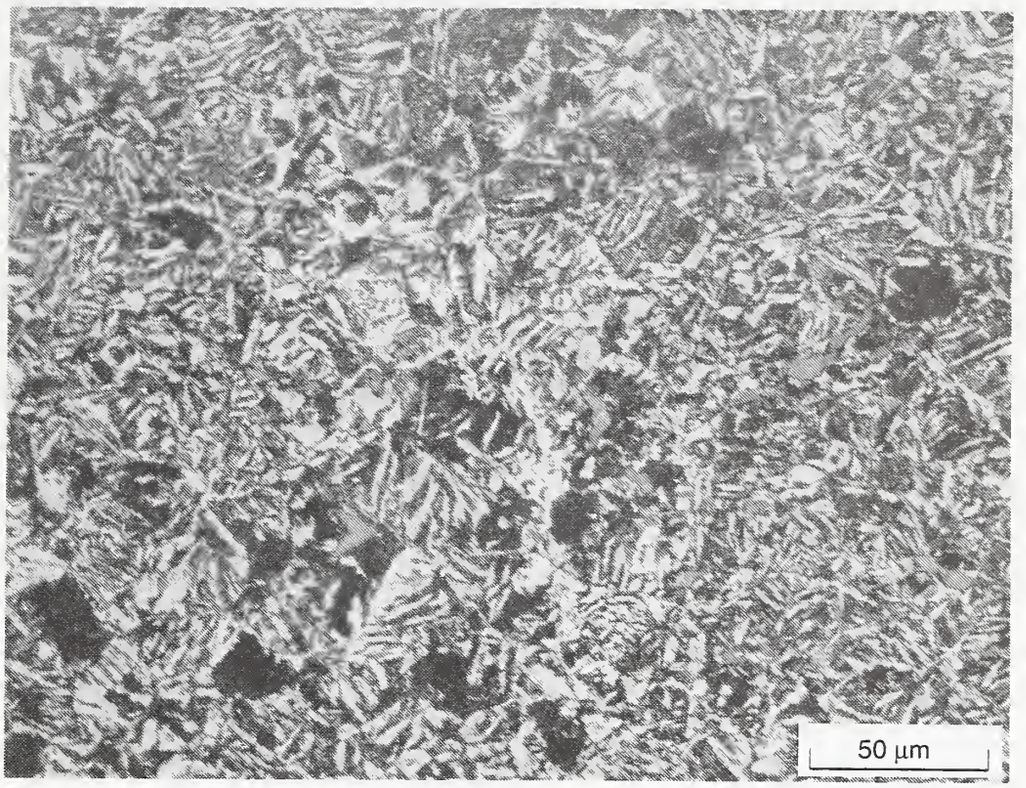

Figure 14. Microstructure of a laboratory specimen (d2 condition) with a cooling time of 170.8 s to cool from 800 to 500°C. The ASTM austenite grain size number is 6.

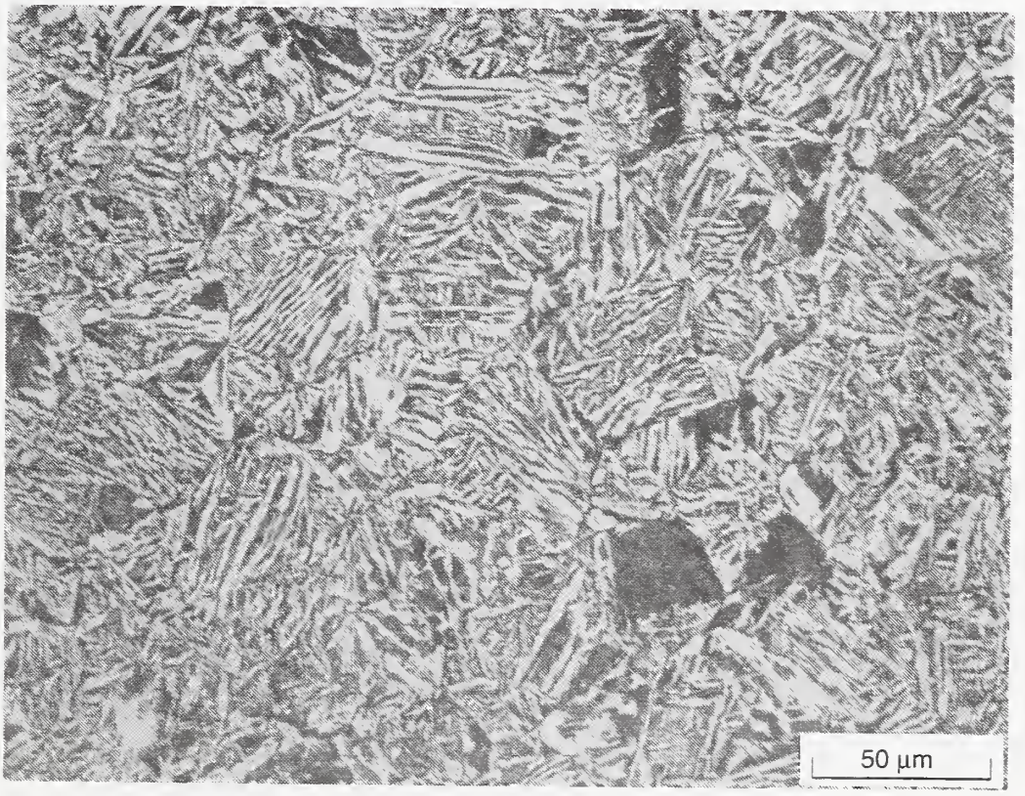

Figure 15. Microstructure of a laboratory specimen (d3 condition) with a cooling time of 129.2 s to cool from 800 to 500°C. The ASTM austenite grain size number is 5.5.

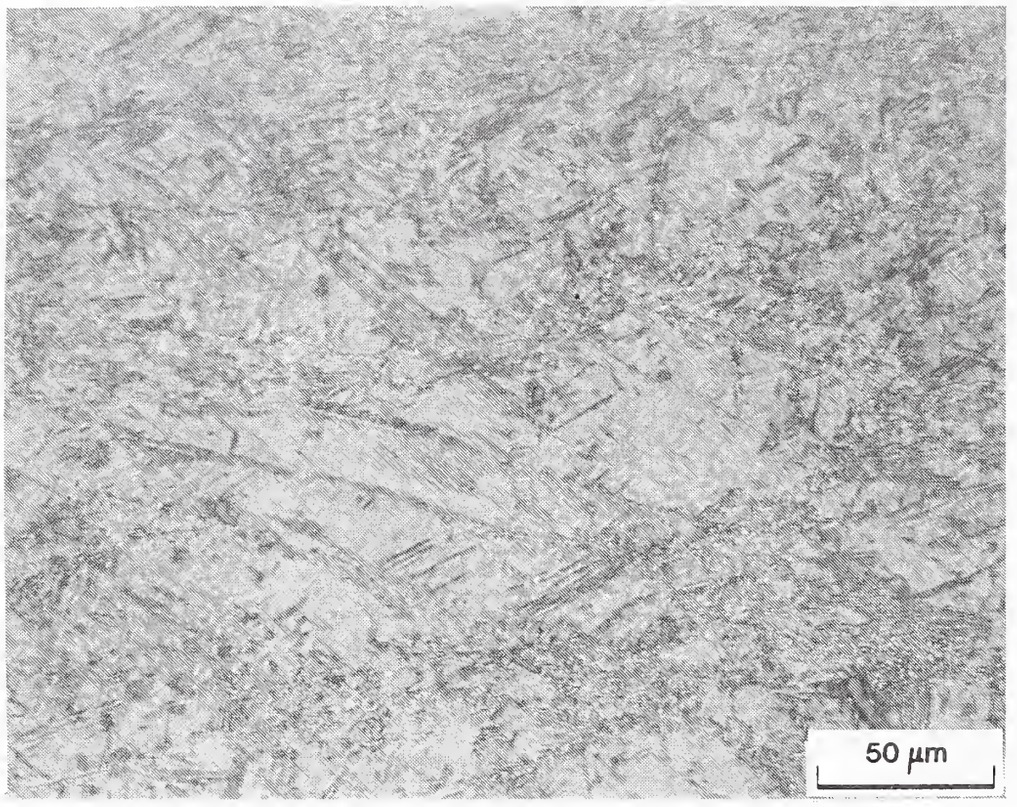

Figure 16. Microstructure of a laboratory specimen after compressed 50% at 900°C. The cooling time from 800 to 500°C is 14.6 s. The banded structure is a result of transformation from flattened nonrecrystallized austenite grains.

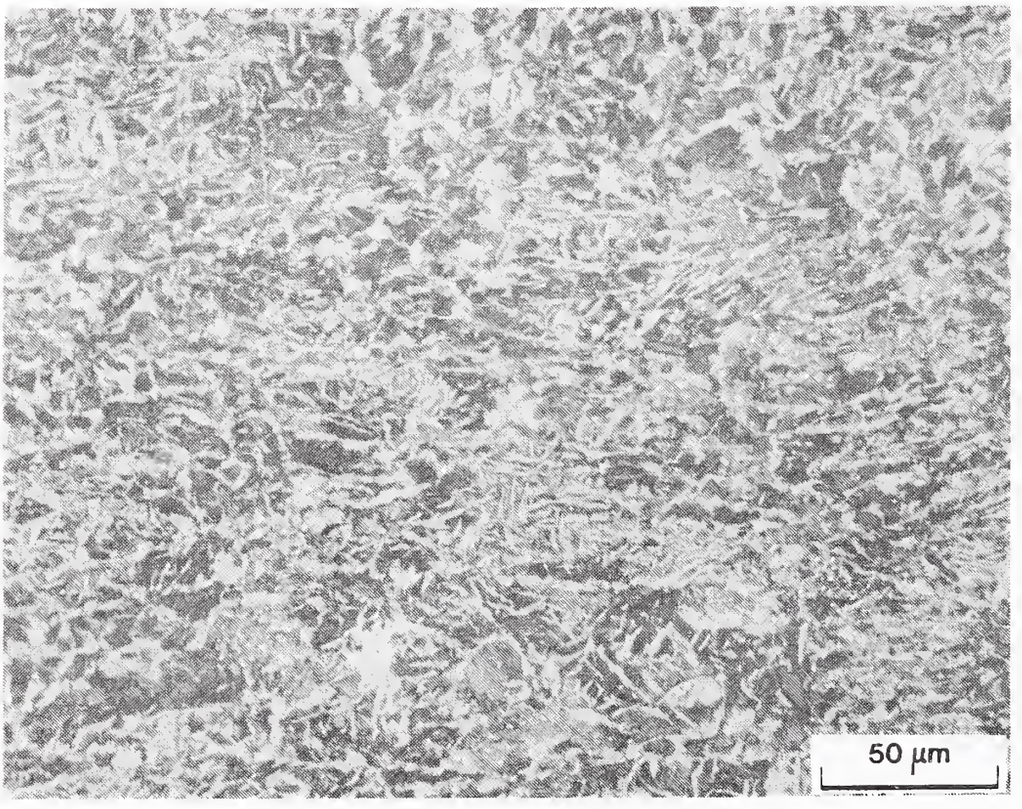

Figure 17. Microstructure of a laboratory specimen after compressed 50% at 900°C. The cooling time from 800 to 500°C is 189 s. The prior austenite grain boundaries were not well outlined because ferrite nucleated not only along the prior austenite grain boundaries but also within austenite grains.

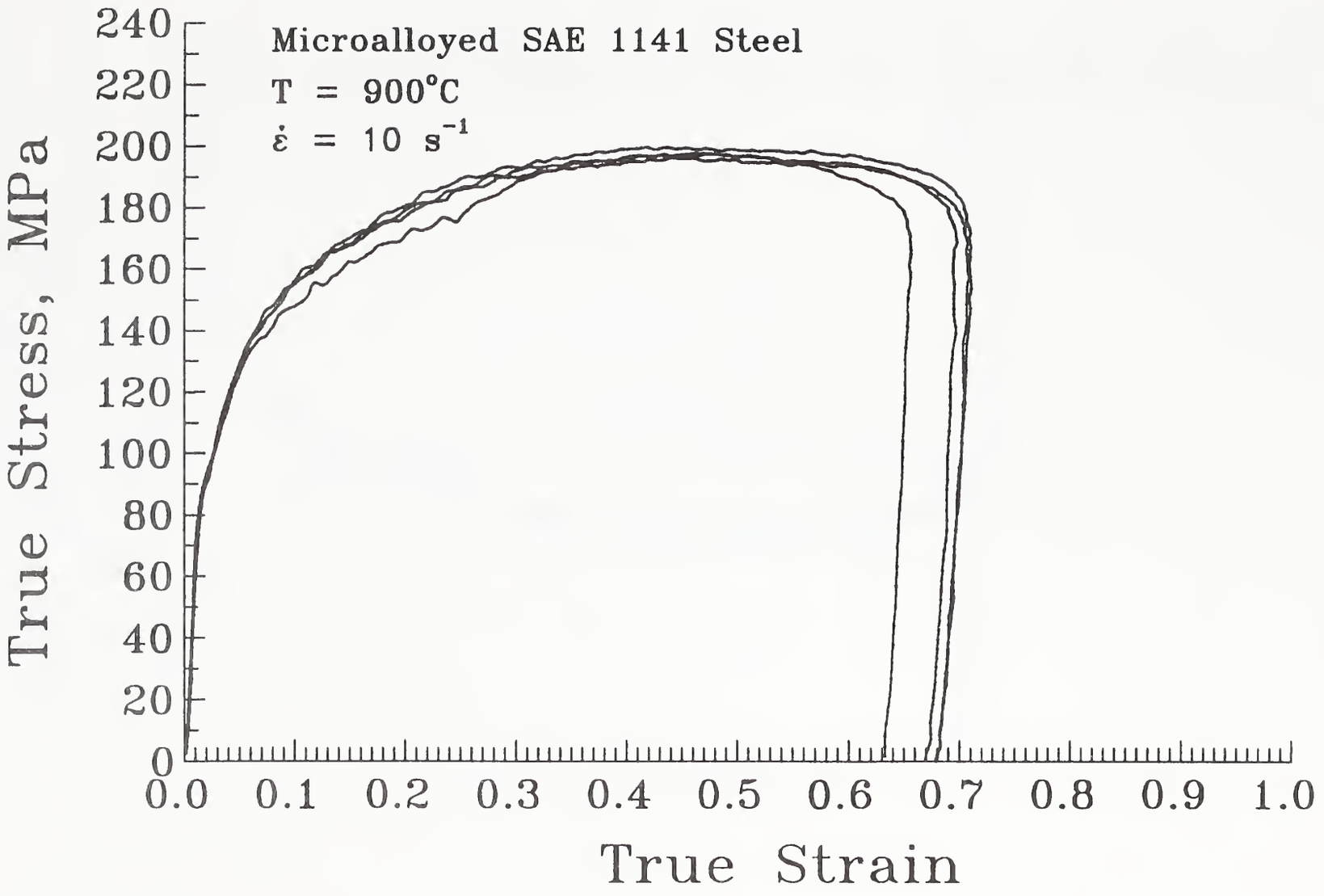

Figure 18. The true stress-true strain curve of the microalloyed SAE 1141 steel tested at 900°C with a strain rate of 10 s^{-1}.

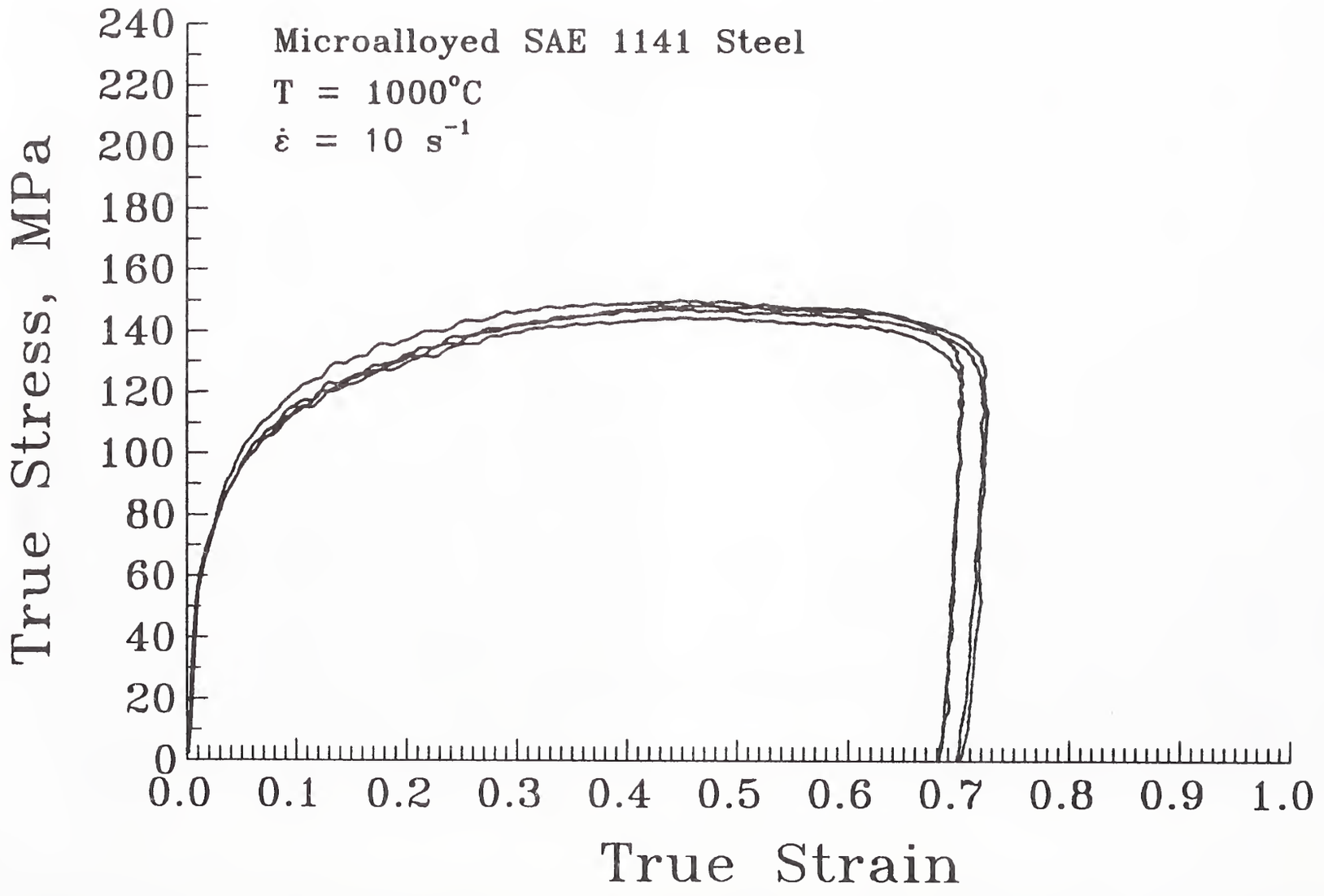

Figure 19. The true stress-true strain curve of the microalloyed SAE 1141 steel tested at 1000°C with a strain rate of 10 s^{-1}.

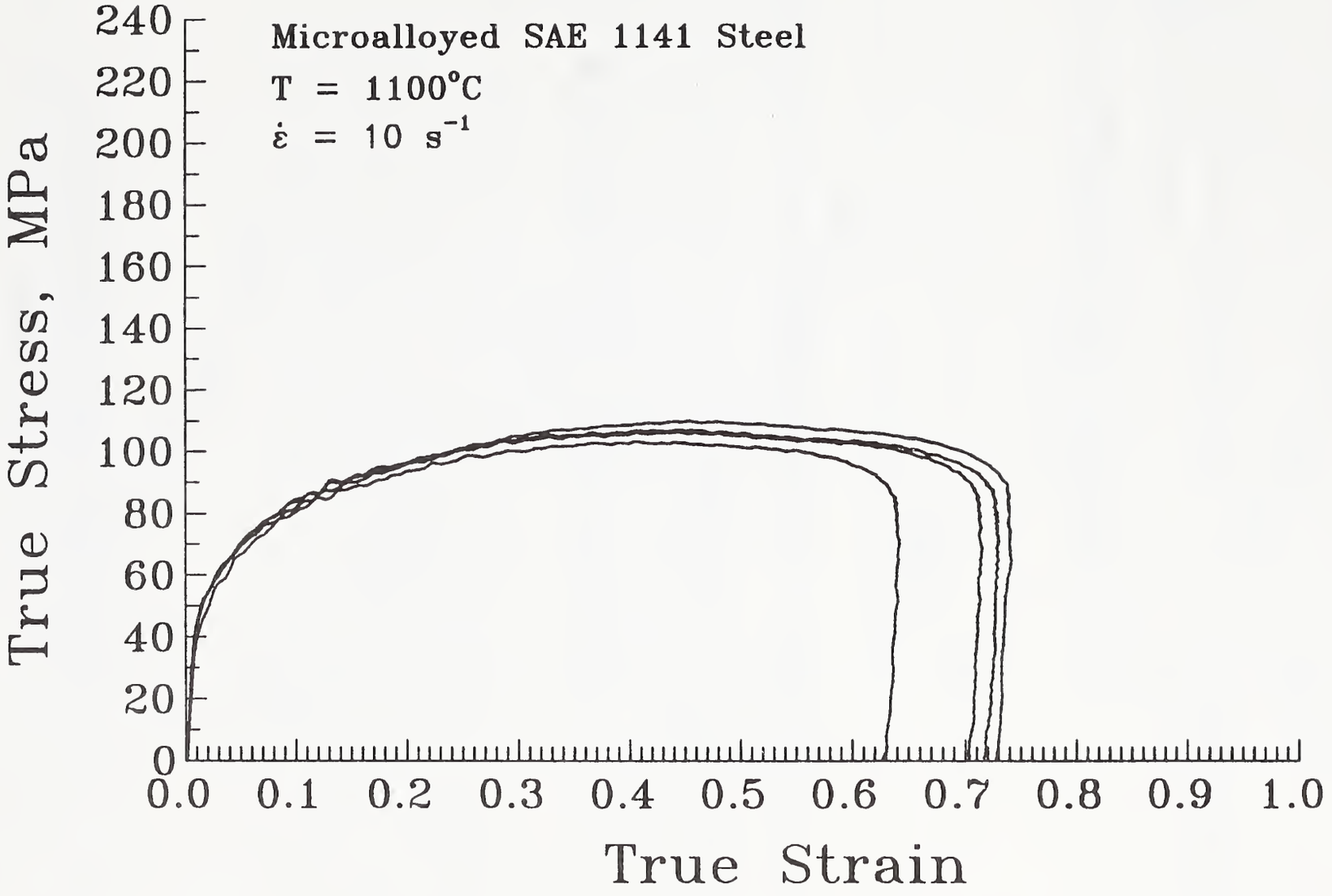

Figure 20. The true stress-true strain curve of the microalloyed SAE 1141 steel tested at 1100°C with a strain rate of 10 s^{-1}.

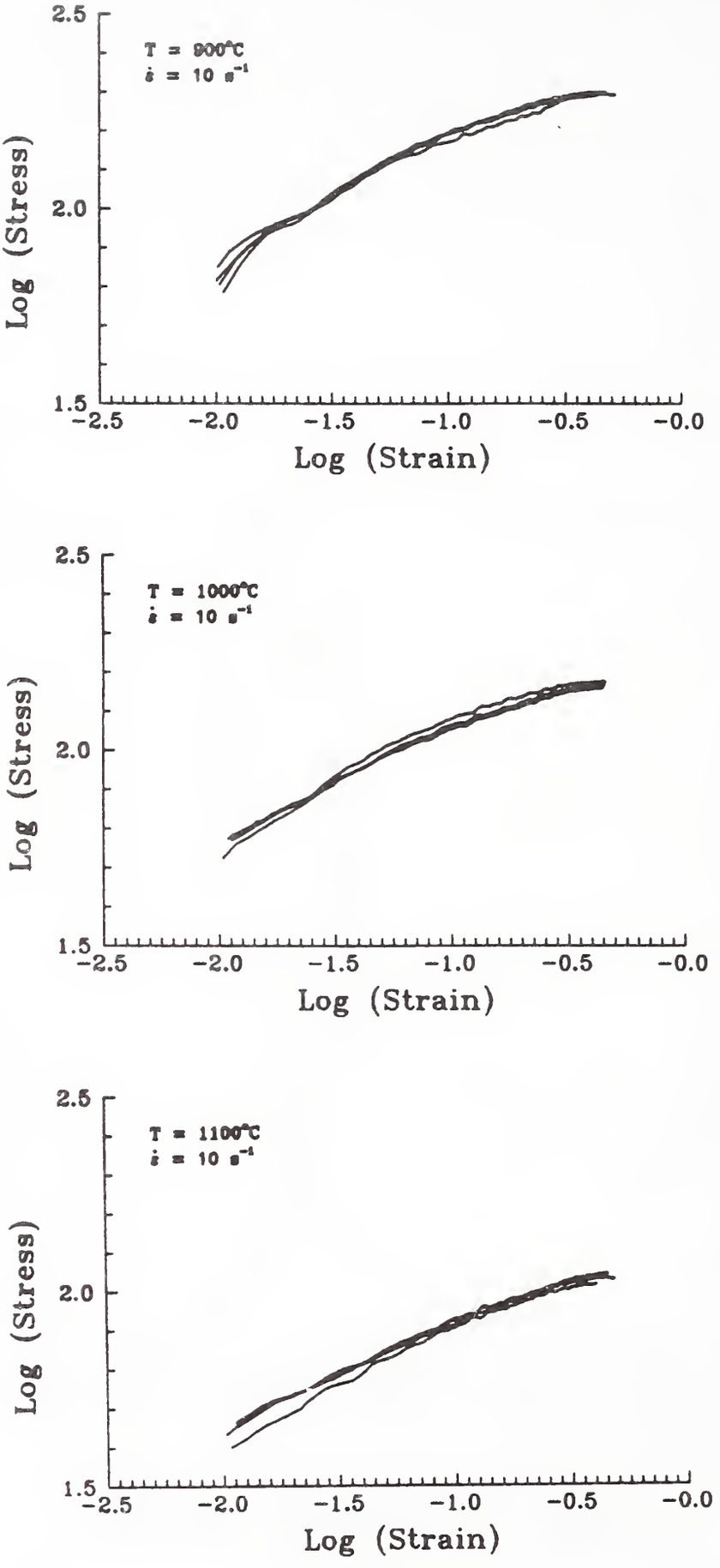

Figure 21. Log (stress)-vs.-log (strain) curves for tests at different temperatures.

-114A
90)

U.S. DEPARTMENT OF COMMERCE
NATIONAL INSTITUTE OF STANDARDS AND TECHNOLOGY

BIBLIOGRAPHIC DATA SHEET

1. PUBLICATION OR REPORT NUMBER
NISTIR 3964

2. PERFORMING ORGANIZATION REPORT NUMBER

3. PUBLICATION DATE
February 1991

TITLE AND SUBTITLE

Continuous-Cooling Transformation Characteristics and High-Temperature Flow Behavior of Microalloyed SAE 1141 Steel

AUTHOR(S)

i-Wen Cheng and Avinoam Tomer*

PERFORMING ORGANIZATION (IF JOINT OR OTHER THAN NIST, SEE INSTRUCTIONS)

U.S. DEPARTMENT OF COMMERCE
NATIONAL INSTITUTE OF STANDARDS AND TECHNOLOGY
BOULDER, COLORADO 80303-3328

7. CONTRACT/GRANT NUMBER

8. TYPE OF REPORT AND PERIOD COVERED

SPONSORING ORGANIZATION NAME AND COMPLETE ADDRESS (STREET, CITY, STATE, ZIP)

SUPPLEMENTARY NOTES

Guest researcher from Nuclear Research Center-Negev, Beer Sheva, Israel.

ABSTRACT (A 200-WORD OR LESS FACTUAL SUMMARY OF MOST SIGNIFICANT INFORMATION. IF DOCUMENT INCLUDES A SIGNIFICANT BIBLIOGRAPHY OR LITERATURE SURVEY, MENTION IT HERE.)

This report presents the results of a thermomechanical processing (TMP) study on a microalloyed SAE 1141 forging steel. The primary objective of the study is to investigate the effects of deformation temperature on the phase-transformation kinetics and to determine the high-temperature flow characteristics of the steel. One-hit compression tests at a constant true strain rate of 10 s^{-1} were performed with a TMP simulator. Tests were performed at 900, 1000, and 1100 °C.

The results show that flow stress increased with decreasing temperature. In the strain range 0.35 to 0.6, the effect of temperature on the flow stress can be described by the equation, σ (MPa) = 2.93 exp[4944/T (K)]. Continuous-cooling transformation (CCT) diagrams determined following deformation at 1000 and 1100 °C were similar. However, deformation at 900 °C shifted the ferrite-plus-pearlite nose to a shorter time and produced a much finer ferrite-plus-pearlite microstructure. This is because the steel does not recrystallize at 900 °C after deformation imposed in this study. The usefulness of the CCT diagram and the relationship between deformation and austenite recrystallization are discussed.

KEY WORDS (6 TO 12 ENTRIES; ALPHABETICAL ORDER; CAPITALIZE ONLY PROPER NAMES; AND SEPARATE KEY WORDS BY SEMICOLONS)

Continuous-cooling transformation; flow stress; forging steels; microalloyed steels; recrystallization; thermomechanical processing; true stress-true strain curves.

AVAILABILITY

UNLIMITED

FOR OFFICIAL DISTRIBUTION. DO NOT RELEASE TO NATIONAL TECHNICAL INFORMATION SERVICE (NTIS).

ORDER FROM SUPERINTENDENT OF DOCUMENTS, U.S. GOVERNMENT PRINTING OFFICE, WASHINGTON, DC 20402.

ORDER FROM NATIONAL TECHNICAL INFORMATION SERVICE (NTIS), SPRINGFIELD, VA 22161.

14. NUMBER OF PRINTED PAGES
40

15. PRICE

ELECTRONIC FORM